Materials and Devices
An International Scientific Journal
OPEN ACCESS Freely Accessible Scientific Papers.
CA-IP
Managed by scientists for Science - http://co-ac.com

Article type: A-Regular research paper

ZnTe/CdSe type-II core/shell spherical quantum dot under an external electric field

A. Chafai (1,*), I. Essaoudi (1,2), A. Ainane (1,2,3), F. Dujardin (2), R. Ahuja (3)

(1) *Laboratoire de Physique des Matériaux et Modélisation des Systèmes, (LP2MS), Unité Associée au CNRST-URAC 08, University of Moulay Ismail, FSM, B.P. 11201, Meknes, Morocco.*
(2) *LCP-A2MC, Université de Lorraine, Institut de Chimie, Physique et Matériaux, 1 Bd. Arago, 57070 Metz, France.*
(3) *Condensed Matter Theory Group,Department of Physics and Astronomy, Uppsala University, 75120 Uppsala, Sweden.*

Corresponding author : evoachmed@gmail.com

RECEIVED: 23 january 2018 / RECEIVED IN FINAL FORM: 05 april 2018 / ACCEPTED: 06 april 2018

Abstract : We have investigated in the framework of the envelope function approximation and taking into account the dependence of the electron effective mass on radius the energy of an electron inside a ZnTe/CdSe core/shell spherical quantum dot. In order to make the problem more realistic, we describe the conduction band-edge alignment between core and shell materials by a finite height barrier. By applying the Ritz variational principle the effect of the electric field on the electronic states was also examined. Our numerical results show the opportunity to control the energy states position of the charge carriers inside our core/shell nanostructures by controlling the size (core radius, shell thickness) of the nanostructure and the strength of the external electric field.

Keywords : CORE/SHELL MATERIALS, NANOSTRUCTURES, QUANTUM DOTS, ELECTRIC FIELD

Introduction

The world of materials science is witnessing a flagrant change in the exploration of matter at small scale [1]. When the matter is at nanoscales, we are witnessing at improved and advanced properties [2]. Nowadays nanomaterials have become more popular and their applications may be encountered in various fields, such as nanoelectronics, nanophotonics, nanomedicines, nanosensors and so on [3, 4]. A major feature of nanoscaled materials is the quantum confinement effect, which leads to spatial enclosure of the electronic charge carriers within the nanostructure. When the motion of the charge carriers is frozen over all the three spatial directions, then we talk about quantum dots (QDs). We can find in the literature various works about this zero dimensional semiconductors. For example, Montenegro et *al.* [5] applied the variational procedure in the effective-mass approximation to calculate the ground state donor-binding energy and the density of states of donor in spherical GaAs-(Ga,Al)As QDs, as functions of the QD radii and of the donor position. Bose [6] found that the binding energy decreases as the dot dimension increases and as the impurity moves away from the center. It is also shown that the effect of the nanodot size and the donor position on the binding energy is more pronounced for dots of smaller sizes. Marin et *al.* [7] investigated the ground state energy of excitons inside a micro-spherical crystallites with a finite height potential wall as a function of the particle radius in the strong confinement regime. They have demonstrated that the quantum dot cannot be modelled using an infinite barrier height potential in the strong confinement regime. Other shapes of quantum dots have also been extensively studied essentially cylindrical QDs [8-11], lens QDs [12-14] and pyramidal QDs [15-18].The effect of an external electric field on the ground-state energy of charge carriers inside quantum dot was also studied by several authors. Using a variational method Lien et *al.* [19] have investigated the correlation energy of hydrogen impurities in spherical and disc-like quantum dots with parabolic confinements submitted to an external electric field. He et *al.* [20] have applied a non degenerate and degenerate perturbation approach to calculate the correlation energies of the ground and three low-excited states of hydrogenic impurity inside a spherical parabolic-like quantum dot as a function of the confinement strength and the intensity of the applied electric field. Ref. [21] presents a study of the ground state binding energy of an impurity inside quantum dots under external electric and magnetic fields. Using the micro-photoluminescence spectroscopy, the problem of an exciton in a single InGaN quantum dot was treated by Robinson et *al.* [22]. They have found that the quantum-confined Stark effect causes a shift in the exciton energy of more than 5 meV, accompanied by a reduction in the exciton oscillator strength. The shift has both linear and quadratic terms as a function of the applied field. Dujardin et *al*. [23] performed a variational approach to investigate the behavior of an exciton confined in ZnO single quantum disk under lateral electric field. They have shown that the electric field shifts down the excitonic binding energies. In the last decade, semiconductors core/shell quantum dots attracted interest of several researchers owing to their improved properties [25-26]. According to the maximum of the valence band and the minimum of the conduction band is or isn't in the same material we can distinguish three categories of semiconductors core/sell quantum dots [24], type-I, type-II and reverse type-I. Fig.1 gives an overview of the principal categories of core/sell quantum dots. Due to the conduction and valence band profile of type-II core/sell quantum dots, the overlapping of the electrons and holes wave functions is reduced. As a result, one carrier is mostly confined to the core, while the other is mostly confined to the shell. The energy gap in this category of core/shell material ($E_g^{c/s}$) is determined by the energy separation between the conduction band edge of one semiconductor and the valence band edge of the other semiconductor. $E_g^{c/s}$ can be related to the conduction and valenceband energy offsets at the interface by the following equation [27]:

$$E_g^{c/s}=E_g^c-V_v=E_g^s-V_c \quad (1)$$

Where E_g^c and E_g^s are, respectively, the band gaps of semiconductors core and shell. In this case, emission is lower than the band gap of either semiconductor. As a result the emission color is shifted toward spectral ranges.

In the present work, we are concerned with the calculation of the energy state 1s, (n=1, l=0, m=0), of one electron confined in core/shell quantum dot type-II. For this purpose we firstly investigate the case with zero electric field afterwards, we turn up an electric field $\vec{F}$ parallel to the ($\overrightarrow{OZ}$) axis. In the next section we introduce the theoretical formalism, while in section 3 we present our numerical results.

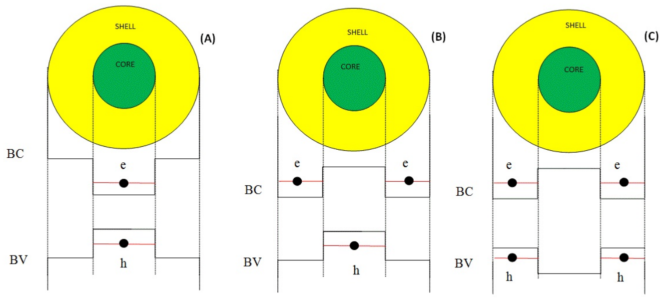

Figure 1: Categories of semiconductors core/sell QD (A) type-I, (B) type-II, (C) reverse type-I.

The model and applied theory

Within the framework of the effective-mass approximation, applying the isotropic and non-degenerate parabolic approximations, taking into account the dependence of the electron effective mass on radius and assuming that the core and shell materials dielectric constants are sufficiently close to ignore the effects of induced surface polarization charges. The stationary Shrödinger equation of a system consisting of an electron inside a core/shell spherical quantum dot submitted to an external electric field can be written as:

$$\left[\frac{d^2}{dr^2}+\frac{2}{r}\frac{d}{dr}+k_i^2-\frac{l(l+1)}{r^2}+\frac{2m_e(r)}{\hbar^2}W\right]\chi_{nl}(r)=0 \quad (2)$$

where the electron effective mass (the square of the wave vector k_i^2) is assumed to be m_1 ($\frac{2m_1}{\hbar^2}\left(U_e-E_e^{10}\right)$) in the core material and m_2 ($\frac{2m_2}{\hbar^2}E_e^{10}$) in the shell material, and W = -q **F**.**r** is the electrostatic energy. It is clear that the presence of the electric field makes the problem more complicated and does not admit any analytical solution, that is why we have applied a variational approach to determine the electron ground state energy, and by analogy to the problem of the quantum wells we chose as our variational wave function:

$$\chi_{10}(r)=\Psi_{10}(r).\exp\left(-\alpha r\cos(\theta)\right), \quad (3)$$

where α is the variational parameter, θ is the angle between the electron position vector and the z-axis and $\Psi_{10}(r)$ is the exact wave function of the same system with zero electric field. Accordingly the energy of the electron 1s under an external electric field is determined variationally by the following expression:

$$E_e^{10}=\min_{\alpha}\left[\frac{\langle\chi_{10}(r)|H_f|\chi_{10}(r)\rangle}{\langle\chi_{10}(r)|\chi_{10}(r)\rangle}\right] \qquad (4)$$

Where H_f is the Hamiltonian of the confined electron under an electric field.

Discussion of the results

We present in this section the results of our numerical calculation performed for ZnTe/CdSe core/shell spherical quantum dot characterized by an electron effective mass $m_{ZnTe}=0.15m_0$ [28] ($m_{CdSe}=0.13m_0$ [29]) in the core (shell) material. First of all, we start our analysis by the case with zero electric field. To this end, and in order to give a detailed investigation of the electronic behavior of an electron confined in our nanostructure we display, in figure 2, the energy ground state versus the core to shell radii ratio R_c/R_s for various inner radius values: R_s = 5 nm, 15 nm, 20 nm, 40 nm, 50 nm, 70 nm. We can easily notice that the energy ground state undergoes a great change by changing the value of R_c and R_s radii. In more detail the energy ground state increases if the size of the nanostructure decreases and for a fixed total size of the nanostructure the energy decreases if the thickness of the shell material T_S increases. We can also find out that the effect of the size of core material on the energy ground state is more pronounced for the small nanostructures. For example the effect of the core size can be easily noticed for small core/shell nanostructure even for a core to shell radius ratio neighboring 0.15 which is very small as compared with large core/shell nanodot in which this effect will manifest only for core to shell radius ratio practically higher than 0.6. This variation of energy vis-a-vis the dimensionality of the nanostructure is intimately related to the quantum confinement effect which is considered as a major feature of nanostructured semiconductors. Because of this effect, researchers can widely and precisely control the electronic energy states of core/shell nanostructures, by the control of both R_c and R_s radius, which leads to a precise control of the optical transitions making them useful for many optoelectronic devices.

The following provides a description of the influence of an external electric field on the electron ground state energy. For this purpose we plot, in figure 3, The energy ground state of an electron confined in core/shell spherical quantum dot versus core to shell radii ratio R_c/R_s for a fixed external radius value R_s =5 nm and various electric field strength values: F=0 kV/cm and 900 kV/cm. We can notice that the effect of the electric field can be almost marginalized for small nanostructures which is in full agreement with the earlier works already existing in literature [30,31]. This can be attributed to the fact that the electron is strongly confined in the shell material in such a way that the distribution of the electron probability density remains symmetric ensuring to the system to keep practically a similar energy to that in the zero electric field.

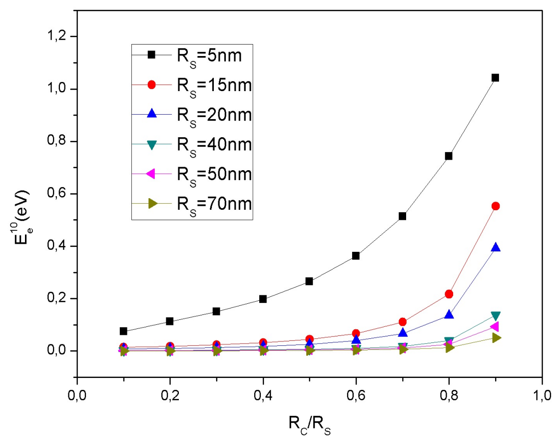

Figure 2: The energy ground state of an electron inside a core/shell spherical quantum dot drawn versus the core to shell radii ratio R_c/R_s for: F=0 kV/cm and R_s = 5 nm (Square symbol), 15 nm (Circle symbol), 20 nm (Up triangle symbol), 40 nm (Down triangle symbol), 50 nm (Left triangle symbol), 70 nm (Right triangle symbol).

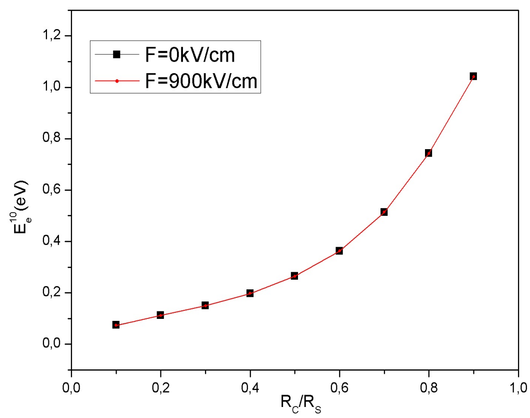

Figure 3: The energy ground state of an electron inside core/shell spherical quantum dot drawn versus core to shell radii ratio R_c/R_s for fixed external radius value $R_s = 5\,nm$ and various values of the electric field strength: F=0 kV/cm (Square symbol), F=900 kV/cm (Circle symbol).

We report in Figure 4(A) the variation of the electron energy ground state versus core to shell radii ratio R_c/R_s for fixed external radius value R_s = 40 nm and various electric field strength values: F=0 kV/cm, 100 kV/cm and 600 kV/cm. In order to understand the behavior of the electron inside core/shell nanostructure under an external electric field we plot in figure 4(B) the stark shift (ΔE=E(0)-E(F)) versus core to shell radii ratio R_c/R_s for fixed external radius value R_s =40nm and various electric field strength values: F=100 kV/cm and 600 kV/cm.

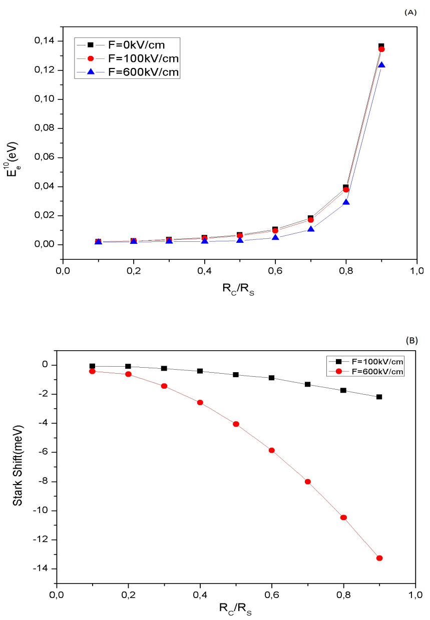

Figure 4: (A) The energy ground state of an electron inside a core/shell spherical quantum dot drawn versus the core to shell radii ratio R_c/R_s for fixed external radius value R_s = 40 nm and various electric field strength values: F=0k V/cm(Square symbol), F=100 kV/cm (Circle symbol), F=600 kV/cm (Up triangle symbol), (B) the stark shift versus R_c/R_s for fixed external radius value R_s = 40 nm and various electric field strength values: F=100k V/cm(Square symbol), F=600 kV/cm (Circle symbol).

We can see that the presence of the electric field perturbs the electronic states of the electron, therefore a modification of the electron energy and the electron probability density are assisted. Indeed, the application of the electric field tends to move the electron probability density in the opposite direction of the applied electric field which leads to break the symmetry of the electron probability density, and as a result the energy is red-shifted. This effect is more pronounced for large nanostructures. That is explained by the fact that in large nanostructure the electron probability density has enough space to move in the opposite direction of the external electric field which lead, by breaking the symmetry of the electron probability density, to the diminution of the electronic ground state energy. In contrast, in small nanostructure case, the electron probability density is too 'tight' so the effect of the electric field is eclipsed by the geometrical confinement effect.

Conclusion

In summary, we have presented the impact of the nanodot size and the external electric field on the electron ground state energy. It is worth remarking that our results are in excellent agreement with the works that already exist in the literature. We have also shown that there are a competition between the effect of confinement and the effect of electric field. Moreover we have found that the application of an external electric field is an additional opportunity to control the energy of charge carriers inside nanostructures core/shell type-II, which is very useful from the application point of view.

Acknowledgements:

This work has been initiated with the support of URAC: 08, the project PPR: (MESRSFC-CNRST) and the Swedish Research Links program dnr-348-2011-7264. The authors would like to thank all the organizations.

REFERENCES

1. T. Pradeep, Nano: The essentials understanding Nanoscience and Nanotechnology. Tata McGraw-Hill Publishing Company Limited, 2007.
2. M. Köhler and W. Fritzsche, Nanotechnology: An Introduction to Nanostructuring Techniques. Wiley-VCH, 2007.
3. B Rogers, J Adam and S Pennathur, Nanotechnology: Understanding small systems. CRC Press, 2015.
4. S Thomas, N Kalarikkal, A.M Stephan, B. Raneesh and A.K. Haghi, ADVANCED NANOMATERIALS: Synthesis, Properties, and Applications. Apple Academic Press, 2014.
5. N. Porras-Montenegro, S.T. Pérez-Merchancano and A. Latgé, J. Appl. Phys. 74 (1993) 7624.
6. C. Bose, J. Appl. Phys. 83 (1998) 3089.
7. J.L. Marín, R. Riera and S A. Cruz, J. Phys.: Condens. Matter. 10 (1998) 1349.
8. P. Schillak and G. Czajkowski, Acta Phys. Pol., A 116 (2009) 871.
9. V.A. Holovatsky, O.M.Voitsekhivska, M.J. Mikhalyova and M.M. Tkach, J. Phys.: Condens. Matter. 12 (2000) 863.
10. R. Charrour, M. Bouhassoune, M. Fliyou, D. Bria and A Nougaoui, J. Phys.: Condens. Matter. 12

(2000) 4817.

11. D.B. Hayrapetyan, E.M. Kazaryan, T.V. Kotanjyan, H.K. Tevosyan, Superlattices Microstruct. 78 (2014) 40.
12. L. Bouzaiene, H. Alamri, L. Sfaxi and H. Maaref, J. Alloys Compd. 655 (2016) 172.
13. A.J. Williamson, L.W. Wang and A Zunger, Phys. Rev. B 62 (2000) 12963.
14. A.H. Rodríguez, and H.Y. Ramírez, Eur. Phys. J. B 66 (2008) 235.
15. M. Grundmann, O. Stier and D. Bimberg, Phys. Rev. B 52 (1995) 11969.
16. M.H. Baier, C. Constantin, E. Pelucchi and E. Kapon, Appl. Phys. Lett. 84 (2004) 1967.
17. J.Kim, L. Wang and A. Zunger, Phys. Rev. B.57 (1998) R9408.
18. M. Sabaeian and M. Shahzadeh, Physica E. 68 (2015) 215.
19. N.V. Lien and N.M. Trinh, J. Phys.: Condens. Matter. 13 (2001) 2563.
20. L. He and W. Xie, Superlattices Microstruct. 47 (2010) 266.
21. F. J. Ribeiro, A. Latgé, M. Pacheco and Z. Barticevic, J. Appl. Phys. 82 (1997) 270.
22. J.W. Robinson, J.H. Rice, K.H. Lee, J.H. Na, R.A. Taylor, D.G. Hasko, R.A Oliver, M.J. Kappers, C.J. Humphreys, and G.D. Briggs, Appl. Phys. Lett. 86 (2005) 213103-213106.
23. F. Dujardin, E. Feddi, A. Oukerroum, J. Bosch Bailach, J. Martínez-Pastor and E. Assaid, J. Appl. Phys. 113 (2013) 064314.
24. P. Reiss, M. Protiere and L. Li, Reviews Core/Shell Semiconductor Nanocrystals. Wiley-VCH, (2009).
25. G.Z. Geng, G.X. Liu, F.K. Shan, A. Liu, Q. Zhang, W.J. Lee, B.C. Shin and H.Z. Wu, Current Appl.Phy. 14 (2014) S2.
26. F. Benhaddou, I. Zorkani, A. Jorio and E. Feddi, Physica B 477 (2015) 100.
27. J. Bang, J. Park, J. Lee, N. Won, J. Nam, J. Lim, B. Chang, H. Lee, B. Chon, J. Shin, J. Park, J. Choi,K. Cho, S. Park,T. Joo and S. Kim, Chem. Mater. 22(2010) 233.
28. V.E. Borisenko and S. Ossicini, What is What in the Nanoworld: A Handbook on Nanoscience and Nanotechnology. Wiley-VCH Verlag & Co. KGaA, 2012.
29. S. Adachi, Properties of Group-IV, III--V and II--VI Semiconductors. John Wiley & Sons Ltd, 2005.
30. I. Essaoudi, B. Stébé, A. Ainane, Phys. Rev. B. 64 (2001) 235311.
31. F. Dujardin, E. Feddi, E. ASSAID, A. Oukerroum, Eur. Phys. J. B 74 (2010) 507.